J Neurophysiol 90: 3874–3887, 2003;
10.1152/jn.00009.2003.

Cerebellar Activation During Copying Geometrical Shapes

Scott M. Lewis,[1,2] Trenton A. Jerde,[1,3,4] Charidimos Tzagarakis,[1,5] Maria-Alexandra Georgopoulos,[1,6] Nikolaos Tsekos,[6,7] Bagrat Amirikian,[1,5] Seong-Gi Kim,[6,7] Kâmil Uğurbil,[6,7] and Apostolos P. Georgopoulos[1,2,4,5,8]
[1]*Brain Sciences Center, Minneapolis Veterans Affairs Medical Center, Minneapolis 55417;* [2]*Department of Neurology, University of Minnesota Medical School, Minneapolis 55455;* [3]*Graduate Program in Neuroscience and* [4]*Center for Cognitive Sciences, University of Minnesota, Minneapolis 55455;* [5]*Department of Neuroscience,* [6]*Department of Radiology,* [7]*Center for Magnetic Resonance Research, and* [8]*Department of Psychiatry, University of Minnesota Medical School, Minneapolis, Minnesota 55455*

Submitted 6 January 2003; accepted in final form 27 April 2003

Lewis, Scott M., Trenton A. Jerde, Charidimos Tzagarakis, Maria-Alexandra Georgopoulos, Nikolaos Tsekos, Bagrat Amirikian, Seong-Gi Kim, Kâmil Uğurbil, and Apostolos P. Georgopoulos. Cerebellar activation during copying geometrical shapes. *J Neurophysiol* 90: 3874–3887, 2003; 10.1152/jn.00009.2003. We studied functional MRI activation in the cerebellum during copying 9 geometrical shapes (equilateral triangle, isosceles triangle, square, diamond, vertical trapezoid, pentagon, hexagon, circle, and vertical lemniscate). Twenty subjects were imaged during 3 consecutive 45-s periods (rest, visual presentation, and copying). First, there was a positive relation between cerebellar activation and the peak speed of individual movements. This effect was strongest in the lateral and posterior ipsilateral cerebellum but it was also present in the paramedian zones of both cerebellar hemispheres and in the vermis. A finer grain analysis of the relations between the time course of the blood oxygenation level–dependent activation and movement parameters revealed a significant relation to hand position and speed but not to acceleration. Second, there was a significant relation between the intensity of voxel activation during visual presentation and the speed of the upcoming movement. The spatial distribution of these voxels was very similar to that of the voxels activated during copying, indicating that the cerebellum might be involved in motor rehearsal, in addition to its role during movement execution. Finally, a factor analysis of the intensity of activated voxels in the ipsilateral cerebellum during copying (adjusted for the speed effect) extracted 3 shape factors. Factor 1 reflected "roundness," factor 2 "upward pointing," and factor 3 "pointing (up or down) and elongation." These results link cerebellar activation to more global, spatial aspects of copying.

INTRODUCTION

The role of the cerebellum in motor function (reviewed in Brooks and Thach 1981; Gilman et al. 1981) is well established. In studies designed to investigate the relations of cerebellar cell activity to movement parameters, clear relations to the speed of movement were found with respect to simple spike activity (i.e., Purkinje cell activity evoked by mossy fiber inputs) (Mano and Yamamoto 1980; see Ebner 1998 for a review). Other studies found relations to joint angle (van Kan et al. 1993), whereas studies of cell activity in the deep cerebellar nuclei found significant relations to hand position, intended direction of movement, and pattern of muscle activity (Thach 1978). Recent studies in behaving monkeys have documented significant relations between simple spike activity and multiple motor parameters (Coltz et al. 1999; Johnson and Ebner 2000). The results of these studies confirmed the prominent relation of the cerebellum to the speed of movement. Such a relation was also found in a PET study in human subjects (Turner et al. 1998). Finally, other studies have focused on the idea that one function of the cerebellum might be to "string together" simple, single-joint movements to produce compound, multijoint movements of the whole arm (Thach et al. 1992). A related but distinct variant of this idea would be that the cerebellum integrates submovements to larger aggregates (e.g., in hand writing where movement segments compose letters).

Apart from movement control, the cerebellum has been implicated in a variety of functions, including sensory function (Gao et al. 1996), timing (Ivry et al. 1988), associative learning (Kim and Thompson 1997), oculomotor learning (Kahlon and Lisberger 2000), skeletomotor learning (Bloedel et al. 1997; Thach 1998), cognitive function (Kim et al. 1994b), complexity of motor planning (Winstein et al. 1997), acquisition of internal models (Imamizu et al. 2000), and so forth. These data lend partial support to their respective ideas, and it is possible that different areas within the cerebellum might serve different functions. This concept is consistent with the varying connectivity patterns of different cerebellar areas, especially with respect to differential projections from the cerebellar nuclei to the cerebral cortex (Asanuma et al. 1983a,b; Dum and Strick 2003); unfortunately, details of the connectivity patterns between cerebellar and cerebral cortices are largely unknown. Therefore the results of a given study will have to be qualified with respect to the area of reference (e.g., vestibulocerebellum, cerebellar hemispheres, etc.), the system studied (e.g., vestibular, oculomotor, skeletomotor), the function investigated (e.g., sensation, learning, cognition, motor), the method used (e.g., single-cell recordings, functional neuroimaging, etc.), and the exact paradigm used (e.g., eye blink, limb movement, etc.).

In the present study, we focused on the function of copying, which constitutes a coordinated visuomotor function with rich spatial and temporal components. We imaged the whole brain in 20 subjects in an attempt to understand the neural mecha-

---

Address for reprint requests and other correspondence: S. M. Lewis, Brain Sciences Center (11B), VAMC, One Veterans Drive, Minneapolis, MN 55417 (E-mail: lewis093@umn.edu).

The costs of publication of this article were defrayed in part by the payment of page charges. The article must therefore be hereby marked "*advertisement*" in accordance with 18 U.S.C. Section 1734 solely to indicate this fact.

nisms of this complex function. We first focused on the cerebellum with 4 aims. The first aim concerned the relations between the cerebellum and movement parameters. Specifically, we wanted to investigate the possible localization of motor effects on alternative cerebellar regions defined as lobules or mediolateral zones, and to delineate the relation of cerebellar activation to particular movement parameters, such as position, speed, and acceleration. The second aim concerned the involvement of the cerebellum in motor set, that is in processes preceding, and preparing for, movement. The third aim concerned the involvement of the cerebellum in more general spatial aspects of copying, as reflected in the kind of shape drawn. For this purpose, we analyzed the data using principal components and factor analysis, after adjusting the data for the speed effect. Finally, we assessed the effect of gender on cerebellar activation. Although there was no a priori reason to expect differences in cerebellar activation, we nevertheless wanted to test for them because this subject was not previously investigated and because, by design (10 women and 10 men imaged), we had adequate statistical power to detect possible differences.

METHODS

Subjects

Twenty healthy, right-handed human subjects [10 women and 10 men, age (mean ± SD) 23.8 ± 6.3 and 27.4 ± 6.7 yrs, respectively] participated in these experiments as paid volunteers. A laterality quotient was calculated using the Edinburgh inventory (Oldfield 1971). The study protocol was approved by the University of Minnesota Institutional Review Board. Informed consent was obtained from all subjects.

Experimental paradigm

Stimuli were generated by a computer and presented to the subjects by a rear-projection screen and a mirror attached to the top of the head-gradient set. The stimuli were 9 shapes (Fig. 1) selected to cover a variety of features, such as the presence or absence of curves, different number of sides, different orientations of the same shape (e.g., square, diamond), and qualitatively distinct shapes (e.g., lemniscate and vertical trapezoid). All shapes had the same surface area and subtended approximately 5 deg of visual angle. Subjects performed three 45-s tasks for each shape in a consecutive order (Fig. 2). In the first task, they fixated a blue spot of light in the center of a black screen; in the second task, the light changed to red and a single white shape appeared around it; in the third task, the light changed to green (a "GO" signal) and the subjects drew the shape continuously by moving an X–Y joystick with their right hand. Subjects were instructed to fixate during all tasks and to draw in the third task. These three tasks were presented in the same order for 2 reasons. First, we wanted to investigate explicitly the presence of motor preparation effects during the visual presentation period, and this could be accomplished only by having this and the copy task in sequence. The second reason was to avoid the possibility of having 2 tasks of the same kind (i.e., fixation, visual or copy) from different shapes be presented immediately after one another.

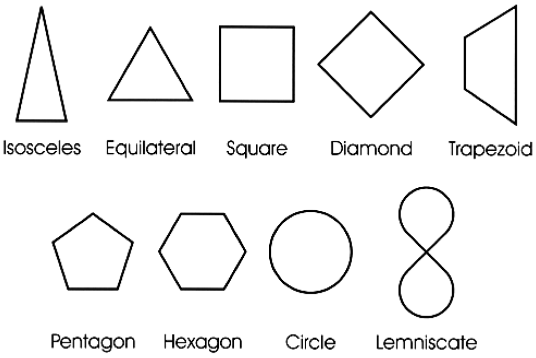

FIG. 1. Nine shapes used.

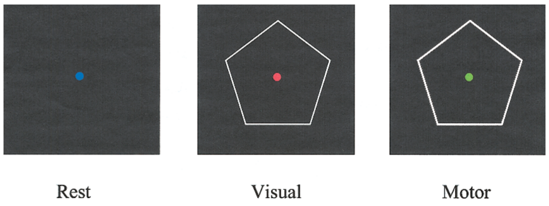

FIG. 2. Three task periods.

Subjects were instructed to copy the shapes counterclockwise at their own speed; no visual feedback was provided. The same sequence was then repeated for another shape, followed by another, until the 9 shapes were shown in a random order; separate randomization was done for each subject. The experiment was controlled by a personal computer, and the X–Y position of the joystick was sampled every 10 ms.

Data acquisition

A 4-tesla whole body system with head gradients and a homogeneous radio frequency coil [Oxford (Oxford, UK)/Varian (Palo Alto, CA)/Siemens (Erlangen, Germany)] was used. A head-support system with several foam pads was used to minimize head movements during the experiment. Multislice axial, sagittal, and coronal anatomic images (T1-weighted) were obtained using a turbo-FLASH sequence with 5 mm slice thickness and in-plane spatial resolution of 1.55 × 1.55 mm. For functional imaging, a T2*-weighted, single-shot echoplanar imaging sequence was used (TE = 25 ms). Imaging planes were axial, with 5 mm slice thickness and in-plane spatial resolution of 3.11 × 3.11 mm. In total, 25–29 slices were collected, covering the whole brain. The acquisition time for a single slice was 100 ms; for a complete multislice image, the repetition time was 3.0 s. Images were collected continuously during the experiment. The duration of each study was 20 min and 15 s. In total, 405 multislice images were collected in each experiment (15 during each task) per subject. The functional magnetic resonance imaging (fMRI) analysis package STIMULATE (version 5.8.1, Center for Magnetic Resonance Research, University of Minnesota Medical School, Minneapolis, MN) was used to process the fMRI images. Images were screened for motion artifacts by measuring variation in the center of mass of the functional images over the entire time course. This measurement was performed separately for the X, Y, and Z coordinates. Subject motion was further assessed by forming a cine loop of the images. Both measurements were performed using the fMRI analysis program STIMULATE and motion correction was performed using automated image registration (Cox and Jesmanowicz 1999). The data acquired covered the whole brain. In this study we present the results of analyses of cerebellar activation; we are currently analyzing the data regarding other brain areas.

Data analysis

TASK PERIODS. Three consecutive task periods were defined for each shape, based on the time of occurrence of behavioral signals described above. Specifically, *1*) the *rest (control) period* was from the onset of the fixation spot until the appearance of the shape; *2*) the *visual presentation period* was from the onset of the shape until the onset of the GO signal; and *3*) the *copying (motor) period* was from the onset of the GO signal until the disappearance of the shape. As mentioned above, each one of these time periods was fixed to 45 s.

SEGMENTATION OF MOVEMENT TRAJECTORIES. The coordinates of the joystick position during the performance of the task were recorded with a sampling rate of 100 Hz. The $x(t)$, $y(t)$ components of the movement trajectories as a function of time t were computed using a cubic spline smoothing algorithm implemented in the IMSL Math Library Package (Visual Numerics, Houston, TX). The speed profile $v(t)$ of a given trajectory was obtained by differentiating the coordinates of the smoothed trajectory with respect to time: $v(t) = \sqrt{\dot{x}^2 + \dot{y}^2}$. The acceleration profile $a(t)$ was obtained by, first, cubic spline smoothing of $v(t)$, and then differentiating it with respect to t. A given trajectory was divided into a series of S segments with breaking points $\{x(t_s), y(t_s)\}$ ($s = 0, 1, \ldots, S$) corresponding to consecutive minima on the speed profile $v(t)$; an example is illustrated in Fig. 3. The time t_s at which velocity reached its minimum was defined from the following conditions: $a(t_s) = 0$, $\dot{a}(t_s) > 0$. Such a minimum-speed segmentation procedure occasionally produced very small segments attributed to the "drawing jitter." Therefore all speed profiles were visually screened and such jitter segments were eliminated by fusing them with corresponding neighboring segments. Finally, the signed angle change (i.e., clock- or counterclockwise) between successive segments ("intersegment angular change") was also calculated.

From these data, descriptive statistics were computed for the following measures of the 45-s copying period of each subject and shape: *1*) number of shapes drawn, *2*) average speed per shape, *3*) number of segments, *4*) average segment length, *5*) average peak segment speed, *6*) average absolute peak segment acceleration, and *7*) average absolute intersegment angular change. It should be noted that the "segments" in the measure above are those defined in the preceding paragraph and not "geometrical" segments based on the shape. For example, there could be more than 4 segments in the drawing of a square. In addition, we computed the time courses of the position of the joystick and its time derivatives, as follows. Each 45-s copying period consisted of fifteen 3-s periods corresponding to the acquisition time of an image. Because the movement data were sampled and collected every 10 ms, we calculated the average values of the x and y position, velocity, and acceleration for each 3-s period. These values were then used as independent variables in a time-varying linear regression model (see following text).

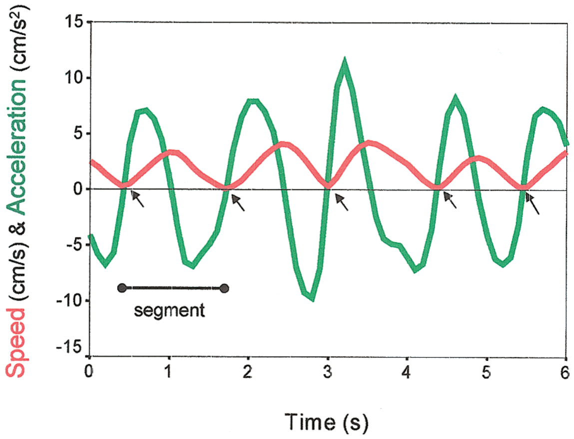

FIG. 3. Illustration of movement segments. Time courses of speed (red) and acceleration (green) during drawing an isosceles triangle are shown. Arrows indicate the demarcation points of movement segments.

fMRI data extraction

The raw data were first log-transformed (using base e) and detrended. Because parametric statistical analyses were performed, it was important to ensure that the data analyzed were normally distributed, that the variance was independent of the mean, and that the effect was linear. These assumptions are key conditions for the validity of any parametric test (e.g., t-test, F-test in an ANOVA or ANCOVA, linear regression, etc.). We evaluated the fulfillment of these conditions by performing a detailed analysis of the data to assess *1*) their frequency distribution (i.e., how close it was to a normal distribution), *2*) the dependency of their SD to the mean, and *3*) the dependency of response on the baseline. The results of these analyses are reported elsewhere (Lewis et al. 2002). Briefly, blood oxygenation level–dependent (BOLD) data showed a strong departure from normality, a strong linear dependency of the SD on the mean, and a proportional response over the baseline. All of these results dictated the need for a logarithmic transformation, which was adopted. Indeed, the log transformation symmetrized the distribution, stabilized the variance, and linearized the effect.

The detrending was necessitated by the presence of time trends; control and task periods were linearly detrended separately after the log transformation. Several measures were then extracted from the data for subsequent statistical analyses using 2 major approaches: one based on regions of interest (ROIs) and the other based on activated voxels, as follows.

ROI ANALYSIS. In every image in which it appeared, the cerebellum was divided into 3 ROIs: the right (ipsilateral) and the left (contralateral) cerebellar hemispheres and the midline; an example is shown in Fig. 4. The ROI for each hemisphere included the lobulus quadrangularis, lobulus simplex, lobulus semilunaris superior, lobulus semilunaris inferior, lobulus gracilis, lobulus biventer, tonsilla cerebelli, and flocculus; the ROI for the midline included the lobulus centralis, culmen, declive, folium, tuber, pyramis, uvula, and nodulus. For each task and ROI, the fMRI signal was averaged, after excluding the first 2 images to ensure a steady hemodynamic state had been reached. Thus 1,620 total values were calculated (20 subjects × 3 tasks × 9 shapes × 3 ROIs = 1,620).

VOXEL ANALYSIS. Two kinds of functional activation maps were generated. One compared the average intensity of each voxel during the visual presentation period to that observed during the control period; the other compared the average intensity of each voxel during the copying period to that observed during the visual presentation period. Our purpose in the latter analysis was not to identify "statistically significant" voxels, but rather to identify those voxels with large changes in BOLD signal, that is, the "peaks of activation." Therefore we did not seek to attach values of statistical significance to a given voxel, but aimed to select the "activated" voxels in a conservative way such that statements concerning their distribution and relations to movement parameters could be examined. A given voxel was deemed "activated" based on a conservative combination of criteria: *1*) for each voxel, the coefficient of variation for the control period could not exceed 5%; *2*) voxel contiguity was required (see following text); and *3*) an average cluster z-score value in the signal change (see following text) of 3 or higher was required. The criterion for the coefficient of variation was used because it has been documented that the coefficient of variation is higher in the vicinity of large vessels as well as outside the brain (Kim et al. 1994a). The z-score values were calculated as follows. First, the mean signal (across time points) during the control (C) and the task (T) periods was calculated. Second, a normalized signal change (S) was computed as: $S = (T - C)/C$. Third, the mean (S_{MEAN}) and SD of positive S in all voxels lying in the brain of a given subject were calculated. Fourth, the value of $S_{\mathrm{MEAN}} + 3\mathrm{SD}$ (i.e., z-score $= 3$) was calculated. The voxel contiguity criterion required the presence of at least 2 contiguous voxels in the same plane sharing a full side and having an

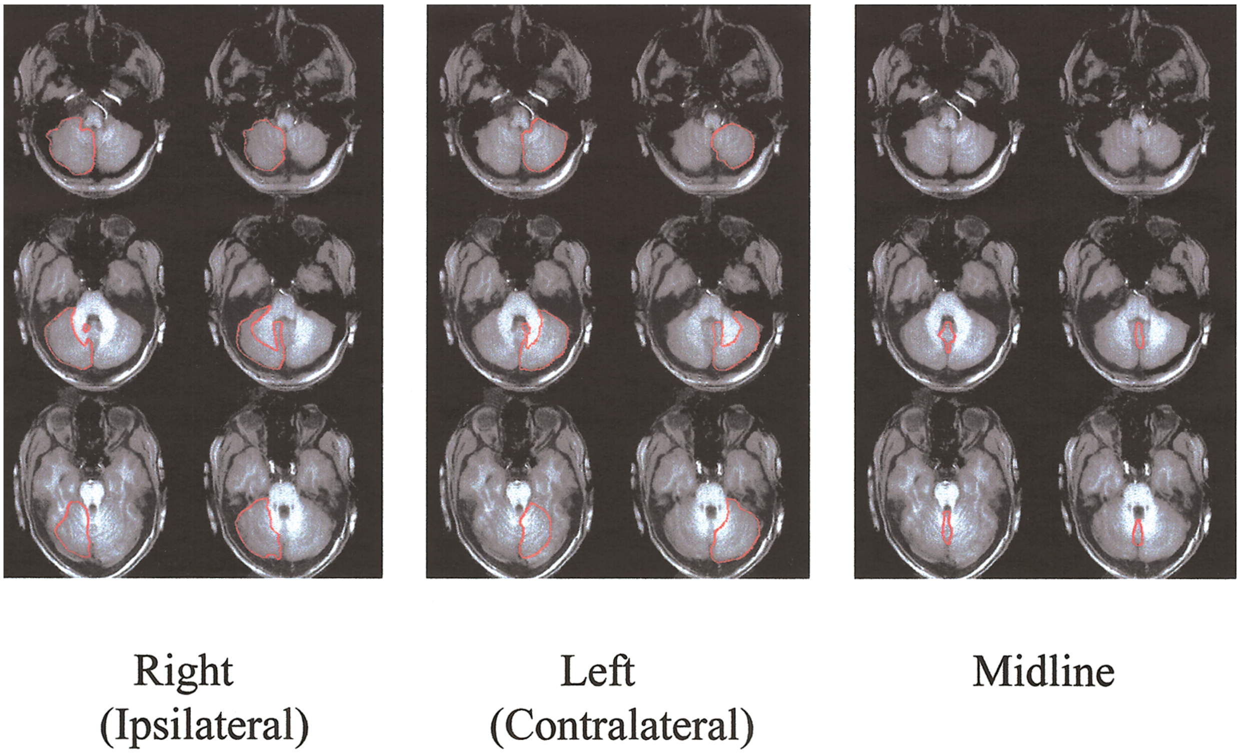

Right (Ipsilateral)

Left (Contralateral)

Midline

FIG. 4. Examples of the 3 cerebellar regions of interest (ROIs).

average z-score of ≥ 3. Finally, each activated voxel was assigned Talairach coordinates (Talairach and Tournoux 1988).

The number k of activated voxels in each of the 3 cerebellar ROIs in each subject, demarcated as described above, was determined in addition to the total number M of voxels in the ROI. Given that ROI size can vary from subject to subject, the ratio $g = k/M$ provided a normalized spatial activation measure.

Anatomical parcellation of the cerebellum

For voxel analysis, we used the atlas of Schmahmann et al. (2000) to parcellate the cerebellar hemispheres into lobules. Because the output of the cerebellar cortex to the deep nuclei is organized along mediolateral zones (Voogd and Glickstein 1998), we also parcellated the cerebellum into 5 mediolateral zones, that is, midline (vermis), paramedian (right, left), and lateral (right, left) zones. The border between the paramedian and lateral zones was placed approximately in the middle of the respective hemisphere; thus the paramedian zone was placed medially to this border. Because the border above may be construed as somewhat liberal, we subdivided the paramedian zone further into 3 parts and statistical analyses were carried out separately for those parts.

General statistical analyses

Standard statistical methods were used to analyze the data (Snedecor and Cochran 1989), including, for example, t-test, ANOVA, ANCOVA, and linear regression. The SPSS 10.1 for Windows (2000; SPSS, Chicago, IL) and the BMDP/Dynamic (1992; BMDP Statistical Software, Los Angeles, CA) statistical packages were used. Unless otherwise noted, we use the terms "statistically significant" or "significant" to denote $P < 0.001$. For ANOVA or ANCOVA, the F-test is the test referred to.

Bootstrapping procedure

Where appropriate, bootstrapping (Efron and Tibshirani 1993) was used to estimate standard errors of regression coefficients. For that purpose, bootstrap samples of $n = 100{,}000$ were generated from the original distribution with replacement and regression coefficients computed for each such sample. From these values, asymptotic standard errors (ASE) were computed and used for statistical significance testing based on the normal distribution.

Time-varying multiple regression analysis

This analysis was used for ROI and voxel analyses and was aimed to determine the relations between the time-varying intensity of cerebellar activation and the corresponding movement parameters. We performed a multiple linear regression analysis in which the ln-transformed BOLD activation in a 3-s period f was the dependent variable and the average position (x, y), velocity ($\dot{x}$, $\dot{y}$), and acceleration ($\ddot{x}$, $\ddot{y}$) of the hand in that period were the independent variables. Because all variables in this model are time courses, it is expected that the errors would be correlated, invalidating the assumption in the ordinary regression model that the errors are uncorrelated. Indeed, preliminary analyses showed that this was the case. This finding necessitated the use of the following model to take this aspect into account

$$f_{t+\tau} = b_1 x_t + b_2 y_t + b_3 \dot{x}_t + b_4 \dot{y}_t + b_5 \ddot{x}_t + b_6 \ddot{y}_t + u_t \quad \tau = 0, 1, 2 \qquad (1)$$

$$f_{t+\tau} = F_{t+\tau} - \bar{F}_v \qquad (2)$$

where $F_{t+\tau}$ is the time-varying BOLD intensity, $\bar{F}_v$ is the average BOLD intensity during the preceding visual presentation period, b_1–b_6 are regression coefficients, and τ is a 3-s time lag; therefore τ values of 1 and 2 mean that movement parameters in a given bin were paired with BOLD values 3 and 6 s later, respectively. The period of analysis began 6 s (i.e., 2 images) after the onset of the copying period and ended at the termination of this period. Thus the total analysis time constituted thirteen 3-s bins, lasting 39 s. The data included within the shifted activation were always within this behaviorally meaningful time period. The last term in the model above is

$$u_t = \rho u_{t-1} + \varepsilon_t \qquad (3)$$

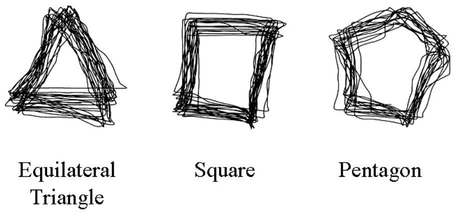

FIG. 5. Examples of copy trajectories from a single subject.

where ε_t is an uncorrelated random error with variance σ^2 and zero mean. The error terms u_t follow a first-order auto-regressive process. The model does not include a constant term because, in all analyses, such a term was not statistically significant. This model was evaluated statistically using the AREG procedure of the SPSS statistical package (see following text).

The t-statistic and its probability level were calculated for each coefficient. Because 6 simultaneous comparisons were performed, the nominal probability level of $\alpha = 0.05$ was adjusted according to the Bonferroni inequality (Snedecor and Cochran 1989) to $\alpha' = 0.05/6 \approx 0.0083$, so that $P < 0.0083$ was considered statistically significant. A significant relation to a parameter was deemed to be present if at least one of the 2 coefficients (corresponding to the $\{X, Y\}$ component of the parameter) was statistically significant. Given that periods of copying were not contiguous, they were separated by a single row of missing data values and the regression was carried out using the exact maximum-likelihood estimation method of the AREG procedure above.

Factor analysis

Factor analysis (Green 1978; Kim and Mueller 1978) was performed on data adjusted for the effect of peak segment speed. Principal-component analysis was the method used for factor extraction and the direct oblimin procedure (delta = 0) with Kaiser normalization was used for factor rotation. The SPSS statistical package (see above) was used for this analysis.

RESULTS

Subject characteristics

The average age between women and men did not differ significantly ($P = 0.232$, t-test), nor did the laterality quotient (Oldfield 1971; $P = 0.178$, t-test).

Behavioral performance

Subjects copied the shapes presented without visual feedback. Examples of movement trajectories for different shapes are shown in Fig. 5. The descriptive statistics of the movement parameters across shapes are shown in Table 1.

Univariate ANOVAs were carried out for all the movement parameters (see METHODS) with shape as a fixed factor. A statistically significant effect was found for the number of shapes drawn, the number of segments, the average segment length, and the average intersegment angular change. No significant effect was found for the average peak segment speed or for the average absolute peak segment acceleration. On the other hand, there was a statistically significant effect of shape on the average speed. These results indicate that the kinetic characteristics of the copies were very similar among shapes, whereas the overall tempo (i.e., average speed per shape) differed among shapes. In fact, curved shapes (i.e., circle and lemniscate) were copied faster than the rest and, of the latter, shapes with more angles tended to be copied more slowly than those with fewer angles.

Table 2 shows the correlations between the various parameters. It can be seen that many parameters were correlated. This poses a potential collinearity problem in studying their relations to BOLD activation. The problem was handled by performing a stepwise multiple linear regression and an extensive collinearity analysis, as described below.

ROI analyses

VISUAL EFFECT. We defined the visual effect as the difference between the signal during the visual presentation period from that observed during the rest period, and assessed this signal in 2 different analyses, separately for each ROI. First, we wanted to know whether there was a statistically significant change in the overall signal [i.e., when averaged across shapes (paired t-test)]. There was no such effect (Fig. 6, *left panel*). Second, we wanted to know whether there was a statistically significant effect of the shape or gender factors (repeated-measures ANOVA). We found no significant effects.

COPY EFFECT. There was a statistically significant increase in the signal of all 3 cerebellar ROIs during the copying period (Fig. 6, *right panel*), compared with that observed during visual presentation alone (paired t-test). This increase differed significantly among the 3 ROIs (Greenhouse–Geisser test in univariate, repeated-measures ANOVA). The signal increase was significantly higher in the ipsilateral ROI compared with either contralateral (×2.26 higher) or midline (×2.05 higher) ROI, whereas it did not differ significantly between the latter 2 ROIs. There was no statistically significant effect of shape on

TABLE 1. *Descriptive statistics for motor parameters (per 45-s copying period)*

Shape	Number of Shape Cycles	Number of Segments	ASL (cm)	APSS (cm/s)	APASA (cm/s2)	AIAC (deg)
Equilateral triangle	14.5 (7.6)	49.6 (21.4)	3.0 (0.6)	7.3 (4.4)	23.5 (22.9)	111.6 (12.2)
Isosceles triangle	13.7 (6.4)	52.3 (20.2)	3.0 (0.7)	7.3 (3.7)	23.4 (19.7)	105.8 (13.2)
Square	11.2 (5.2)	51.8 (18.9)	2.6 (0.7)	6.6 (3.5)	21.4 (17.6)	87.4 (5.1)
Diamond	11.0 (4.7)	52.3 (17.5)	2.5 (0.5)	6.4 (2.7)	21.5 (15.8)	88.4 (3.2)
Trapezoid	9.4 (4.1)	47.0 (16.8)	2.4 (0.5)	5.6 (3.2)	18.6 (16.8)	87.7 (6.7)
Pentagon	9.3 (3.4)	54.1 (17.1)	2.1 (0.5)	6.0 (2.6)	20.5 (14.4)	73.0 (2.9)
Hexagon	8.3 (3.0)	59.0 (19.7)	1.7 (0.4)	5.3 (2.3)	19.5 (13.0)	65.1 (7.0)
Circle	20.4 (10.2)	76.4 (34.3)	2.6 (0.7)	6.7 (3.7)	25.6 (25.2)	102.4 (22.6)
Lemniscate	11.7 (4.6)	76.2 (20.5)	2.3 (0.4)	5.6 (1.7)	20.6 (10.5)	94.7 (15.2)

Values are means ± SD; $n = 20$ subjects per shape. ASL, average segment length; APSS, average peak segment speed; APASA, average peak absolute segment acceleration; AIAC, average intersegment angular change (deg).

TABLE 2. *Correlations between motor parameters*

	Number of Shape Cycles	Number of Segments	ASL (cm)	APSS (cm/s)	APASA (cm/s^2)	AIAC (deg)
Number of shape cycles						
Number of segments	0.793***					
ASL (cm)	NS	−0.171*				
APSS (cm/s)	0.504***	0.513***	0.430***			
APASA (cm/s^2)	0.627***	0.692***	0.185*	0.940***		
AIAC (deg)	0.529***	NS	0.286**	NS	NS	

Values are product-moment (Pearson) correlation coefficients; $n = 20$ subjects × 9 shapes = 180. ASL, average segment length; APSS, average peak segment speed; APASA, average peak absolute segment acceleration; AIAC, average intersegment angular change (deg). NS, not significant; * $P < 0.05$; ** $P < 0.01$; *** $P < 0.001$.

the signal change (copying − visual presentation) for any of the 3 ROIs (repeated-measures ANOVA with shapes as the within-subjects factor and gender as the between-subjects factor, without any covariates, or with speed and/or laterality quotient as covariates; Greenhouse–Geisser test). In addition, neither gender nor the gender-by-shape interaction, nor either of the 2 covariates was statistically significant.

We used a multiple linear regression analysis to find out which, if any, of the motor parameters calculated had a significant effect on the signal change above (dependent variable). There are 2 issues here that needed to be addressed. The first issue concerns the potential collinearity among these parameters, given that several of them were significantly correlated (Table 2). We assessed this problem by performing a detailed analysis of the collinearity effects by calculating the tolerance and variance inflation factor for each variable as well as a number of collinearity diagnostics (2000; SPSS, version 10.1.0, Chicago, IL). Based on the observed correlations (Table 2) and these analyses, we retained 3 (out of 6) motor parameters that had low correlations between them as well as high tolerances and low variance inflation factors in the regression analysis, all of which indicate that they provided independent information. These parameters were the average peak segment speed, the average segment length, and the average absolute intersegment angular change. Entering these parameters as independent variables in the stepwise multiple linear regression model, we found that only the average peak speed had a significant effect on the activation of all 3 ROIs.

The second issue above concerns the possible need for a transformation of the independent variables. We assessed this problem by performing a detailed analysis of the residuals (Draper and Smith 1981). We found that a logarithmic transformation made the average peak segment speed distribution more symmetric, and yielded the highest *F*-score as well as the most unbiased distribution of the residuals, when plotted against the predicted activation value. Because the activation data were also in a log scale, this finding implies a multiplicative model (i.e., a power function), as follows

$$A = kS^b \tag{4}$$

which, taking the logs on both sides, becomes

$$\ln A = \ln k + b \ln S \tag{5}$$

where *A* is the BOLD activation, *k* is a constant, and *S* is the average (per copying period) peak segment speed. The effect of speed was highly significant for the contralateral, ipsilateral, and midline ROI [*t*-test on speed slope in linear regression

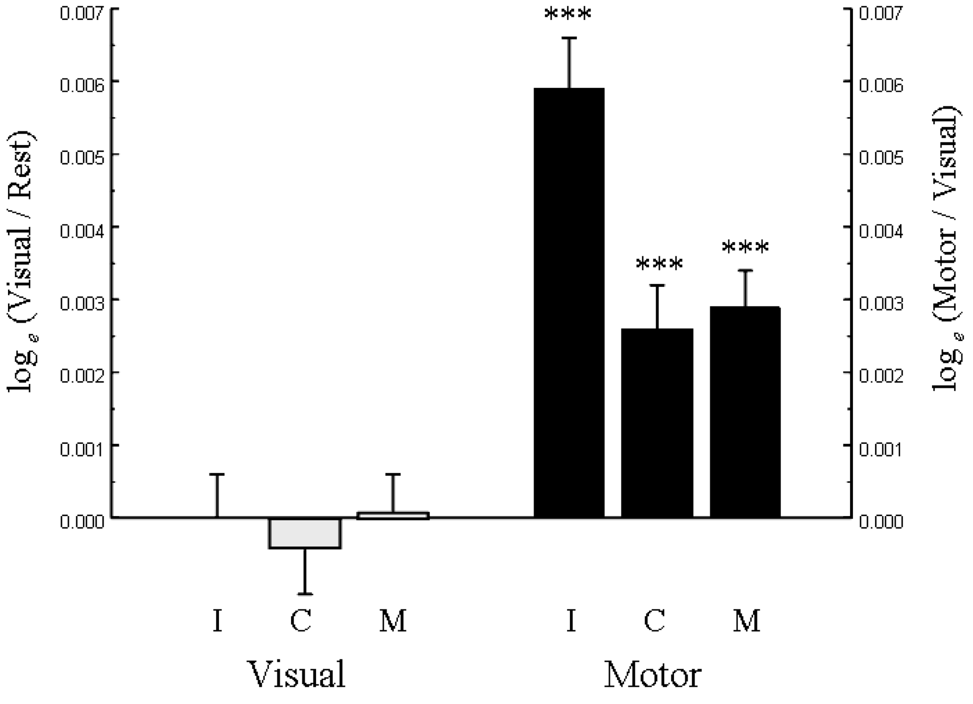

FIG. 6. Analysis of ROIs. Blood oxygenation level–dependent (BOLD) activation (mean + SE, $n = 9$ shapes × 20 subjects = 180) during visual presentation and copying. Asterisks indicate highly statistically significant effects. I, C, M denote ipsilateral, contralateral and midline, respectively.

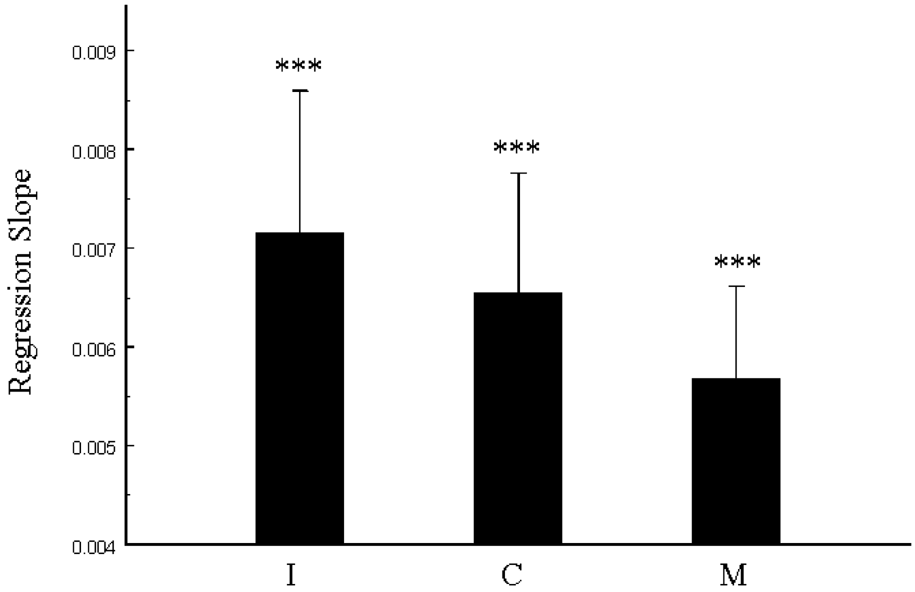

FIG. 7. Effect of log-transformed peak segment speed on BOLD ROI activation during copying. Data are regression slopes (±SE).

analysis (Fig. 7)]. The regression slope was ×1.09 and ×1.26 higher for the right (ipsilateral) ROI than for the left (contralateral) and midline ROIs, respectively.

Voxel analyses

Two different aspects of the activated voxels were analyzed: their intensity and their spatial extent (see METHODS).

VISUAL EFFECT. With respect to the intensity of the activated voxels (Fig. 8, *left panel*), it was significantly higher in the ipsilateral than in the midline ROI (×5.22 higher), and also in the contralateral than in the midline ROI (×4.87 higher), whereas it did not differ significantly between the ipsi- and contralateral ROIs. We did not find any statistically significant effect of the shape or gender factors, or their interaction, on the intensity of the activated voxels contained within the 3 ROIs (repeated-measures ANOVA). Similar results were obtained in the analysis of the normalized extent of activation (see METHODS; for these analyses we used nonparametric statistics, given the known skewed distribution of ratios). Specifically, the extent of activation was significantly greater in the ipsilateral than in the midline ROI (×3.32 higher; Wilcoxon signed-ranks test), and significantly higher in the contralateral than in the midline ROI (×2.99 higher; Wilcoxon signed-ranks test), whereas it did not differ significantly between the ipsi- and contralateral ROIs. We did not find any statistically significant effect of the shape or gender factors, or their interaction, on the extent of activation contained within the 3 ROIs (repeated-measures ANOVA).

COPY EFFECT. With respect to the intensity of the activated voxels (Fig. 8, *right panel*), it was significantly higher in the ipsilateral than in the midline ROI (×5.54 higher; paired *t*-test) and in the contralateral than in the midline ROI (×4.99 higher),

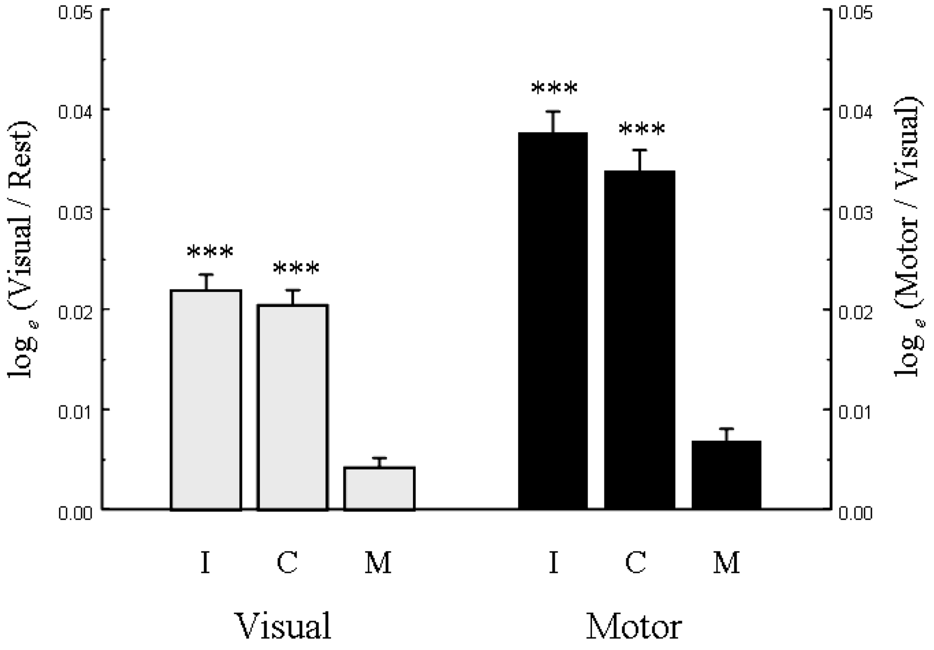

FIG. 8. Voxel analysis. Intensity of activation during visual presentation and copying.

whereas it did not differ significantly between the ipsi- and contralateral ROIs. We did not find any significant effect of shape or gender, or their interaction, on the intensity of the activated voxels within the 3 ROIs (repeated-measures ANOVA). The stepwise multiple linear regression revealed a statistically significant effect only of the average peak segment speed, and only in the right (ipsilateral) ROI ($P = 0.0011$, t-test on regression coefficient of the ln-transformed average peak speed; see *Eq.2* above).

With respect to the extent of activation, it was significantly greater in the ipsilateral than in the midline ROI (×3.11 higher; Wilcoxon signed-ranks test) and in the contralateral than in the midline ROI (×2.47 higher); it was also marginally greater in the ipsi- than in the contralateral ROI ($P = 0.047$, ×1.26 higher). There was a significant effect of the shape factor on the extent of activated voxels for the ipsilateral ($P = 0.006$, Friedman test in one-way ANOVA) and contralateral ($P = 0.033$, same test) ROI; no significant effect was found in the midline ROI, and no significant effects of gender were observed in any ROI (Wilcoxon signed-ranks test). Finally, we examined the relation between the normalized extent of activation and the ln-transformed average peak speed by calculating the nonparametric Spearman correlation coefficient. We found a significant correlation for the ipsilateral ROI ($\rho = 0.2$, $P = 0.007$) but not for the contralateral or the midline ROI. No significant relations were found for other movement parameters (segment length, intersegment angular change) in any of the 3 ROIs.

COMPARISON OF VISUAL AND COPY EFFECTS. With respect to the intensity of the activated voxels, the copy effect was consistently (across areas) and significantly (for the ipsi- and contralateral cerebellum) greater than the visual effect (paired t-test). Specifically, it was ×1.72 ($P < 0.001$), ×1.66 ($P < 0.001$), and ×1.62 ($P = 0.09$) greater for voxels contained in the ipsilateral, contralateral, and midline cerebellum, respectively. With respect to the extent of activation, it was also consistently greater in the copy than in the visual condition in the ipsilateral (×1.38, $P = 0.003$, Wilcoxon signed-rank test), contralateral (×1.22, $P = 0.059$), and midline cerebellum (×1.47, $P = 0.148$). Finally, we compared the effects of the peak segment speed on the intensity of the activated voxels in the visual and motor copy conditions. As mentioned above, a significant effect was found for copying only in the ipsilateral cerebellum; therefore we performed the same regression analysis in this region for the visually activated voxels. The rationale for this analysis was that this "visual" activation might, in fact, reflect motor rehearsal of the upcoming copying, or a motor preparation similar, for example, to that observed in the motor cortex during the delay period of an instructed delay task (Georgopoulos et al. 1989). This idea would be supported if a significant relation were to be found between the intensity of the visually activated voxels and the peak segment speed during the ensuing copying period. Indeed, there was a highly significant positive relation between these variables ($P = 0.007$, t-test on the regression slope). The slope found during copying was ×1.61 higher than that found during visual presentation. This suggests the presence of an "attenuated" motor signal during the visual presentation period.

Location of activated voxels

Activated voxels were distributed throughout the cerebellum. Descriptive statistics for the Talairach coordinates of the voxels activated during the visual presentation (with respect to rest) and during the motor copying (with respect to the visual presentation) are given in Table 3. It can be seen that in all categories the visual and motor distributions were very similar; they did not differ significantly. With respect to cerebellar lobules, the distributions were very similar for motorically and visually activated voxels (Fig. 9), and between the right and left side for either kind, with highly significant correlation coefficients exceeding 0.944.

Localization of motor copying effect

As shown in Table 4, we parcellated the cerebellar cortex into subareas according to the recent atlas of Schmahmann et al. (2000). We were interested to find out whether the relation to the peak segment speed observed for all the ROIs and for the average intensity of activated voxels could be localized in a particular subarea. We found the following (Table 5). First, there was a highly significant relation to speed for the cerebellar midline and for all lobules of the ipsilateral (right) hemisphere, except for lobules I–VI. Second, no significant effects were found in the contralateral (left) hemisphere, except for possibly marginal effects in lobules VIIB–X. Third, there was a gradient of increasingly stronger effects (as judged by the magnitude of the regression slope) from anterior to posterior; specifically, the slope was greater for lobules VIIB–X than for Crus I and II. The effect in the midline was also strong. With respect to mediolateral zones, the strongest effect was observed in the lateral ipsilateral zone where the slope and the significance level were highest. In addition, there was a relatively

TABLE 3. *Descriptive statistics of the Talairach coordinate distributions of the activated voxels for the conditions stated*

	Mean	SD	Min	Max	*n*
Visual, Ipsilateral					
Right/Left	−24	11	−48	0	582
Posterior/Anterior	−57	16	−94	−20	582
Superior/Inferior	−32	10	−4	−50	582
Visual, Contralateral					
Right/Left	24	11	1	53	539
Posterior/Anterior	−58	16	−91	−26	539
Superior/Inferior	−33	10	−9	−51	539
Visual, Midline					
Right/Left	0	4	−7	8	44
Posterior/Anterior	−63	11	−81	−36	44
Superior/Inferior	−25	12	−5	−45	44
Motor, Ipsilateral					
Right/Left	−24	11	−51	−1	833
Posterior/Anterior	−56	18	−93	−17	833
Superior/Inferior	−33	11	−5	−49	833
Motor, Contralateral					
Right/Left	24	10	1	48	647
Posterior/Anterior	−58	16	−94	−21	647
Superior/Inferior	−31	10	−2	−49	647
Motor, Midline					
Right/Left	−1	4	−9	6	67
Posterior/Anterior	−64	7	−78	−50	67
Superior/Inferior	−27	12	−1	−44	67

Left, Anterior, and Superior are positive numbers; Right, Posterior, and Inferior are negative.

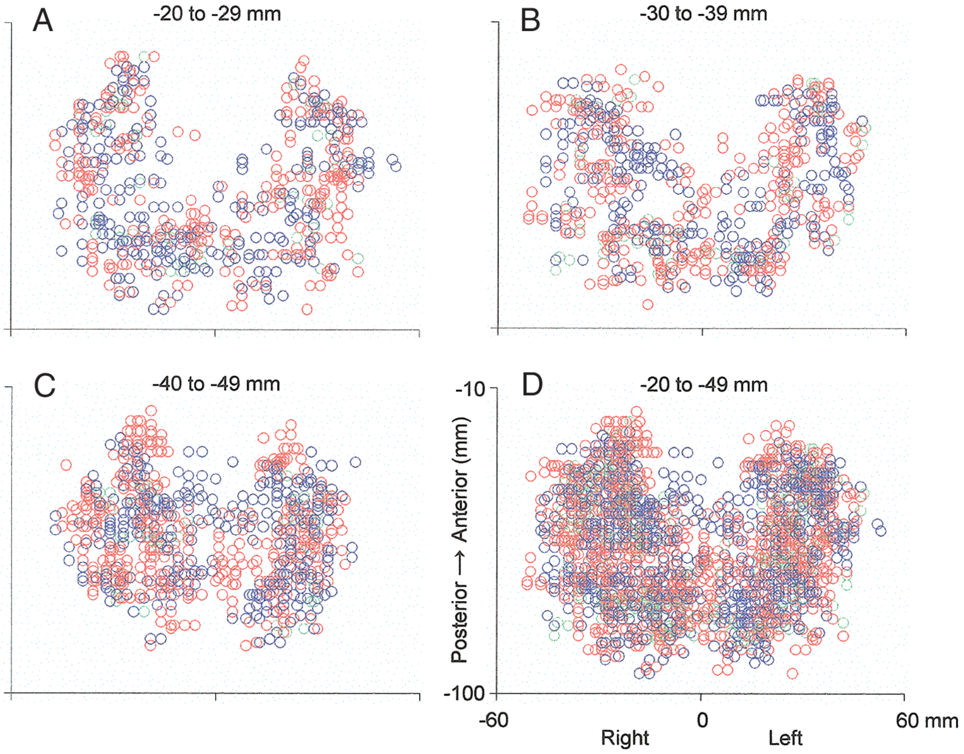

FIG. 9. Overlapping distributions of visually (V; blue circles) and motorically (M; red circles) activated voxels; green circles correspond to voxels activated in both conditions. Diameter of each ellipse is 3 mm, which corresponds to the side of the square voxel acquired. (Ellipses were used for better visualization.) Data from 3 consecutive 10-mm-thick slices are shown, from most superior (*A*) to most inferior (*C*); data from slices *A–C* are combined in *D*. Numbers of voxels shown are as follows: *A*: V = 360, M = 372; *B:* V = 315, M = 409; *C*: V = 377, M = 526; *D*: V = 1,008, M = 1,307. Data are from all subjects.

weak effect in the paramedian zones of both hemispheres and the midline (Table 5). We then assessed this effect for each of 3 subdivisions of the paramedian zone for each hemisphere (see METHODS). We found that the effect was statistically significant in the most medial subdivision in the left (contralateral) hemisphere, whereas it was statistically significant in the 2 more lateral subdivisions in the right (ipsilateral) hemisphere. Finally, no significant effect was observed for the lateral zone of the contralateral hemisphere.

TABLE 4. *Location of activated voxels (counts and percentages) with respect to subdivisions of the cerebellar cortex*

	MV		VR	
	R + L	% of Total	R + L	% of Total
Culmen	13	0.8	6	0.5
Declive	8	0.5	17	1.5
Folium	4	0.3	1	0.1
Pyramis	12	0.8	5	0.4
Tuber	0	0.0	2	0.2
Uvula	30	1.9	13	1.1
I–V	21	1.4	18	1.5
VI	147	9.5	141	12.1
Crus I	463	29.9	382	32.8
Crus II	517	33.4	357	30.6
VIIB	106	6.9	60	5.2
VIII A and B	28	1.8	28	2.4
IX, X	198	12.8	135	11.6
Total	1547	100	1165	100

	MV				VR			
	Right	% of Total	Left	% of Total	Right	% of Total	Left	% of Total
I–V	12	1.4	9	1.4	5	0.9	13	2.4
VI	71	8.5	76	11.7	65	11.2	76	14.1
Crus I	233	28.0	230	35.5	206	35.4	176	32.7
Crus II	290	34.8	227	35.1	182	31.3	175	32.5
VIIB	61	7.3	45	7.0	29	5.0	31	5.8
VIII A and B	22	2.6	6	0.9	11	1.9	17	3.2
IX, X	144	17.3	54	8.3	84	14.4	51	9.5
Total	833	100	647	100	582	100	539	100

MV, voxels activated during the motor period (with respect to the visual presentation period); VR, voxels activated during the visual presentation period (with respect to the rest period); R, right; L, left. Culmen to uvula, cerebellar vermis (midline); I–X, cerebellar hemispheres.

TABLE 5. *Localization of motor effects to lobules and lateral zones of the cerebellar cortex during the copying period*

Hemisphere	Lobule	Slope (b)	ASE	z	P
Left	I–VI				NS
Left	Crus I				NS
Left	Crus II				NS
Left	VIIB, VIII A and B				NS
Left	IX, X				NS
Right	I–VI				0.19
Right	Crus I	0.039	0.014	2.77	0.006
Right	Crus II	0.046	0.014	3.27	0.001
Right	VIIB, VIII A and B	0.068	0.027	2.56	0.01
Right	IX, X	0.065	0.018	3.53	0.0004
Hemisphere	**Zone**	**Slope (b)**			**P**
Left	Lateral				NS
Left	Paramedian	0.019	0.007	2.71	0.007
	Vermis (midline)	0.063	0.02	3.15	0.002
Right	Paramedian	0.027	0.008	3.37	0.0008
Right	Lateral	0.071	0.017	4.17	0.00003

The values shown are results of a linear regression analysis ($\ln A = \ln k + b \ln S$, where A is the BOLD activation, k is a constant, and S is the average (per copying period) peak segment speed). ASE, asymptotic standard error of b calculated by bootstrapping (bootstrap sample size = 100,000; see METHODS). The values for P are probability levels for rejecting the null hypothesis that $b = 0$ (normal deviate based on ASE; two-tailed).

Time course analysis

We carried this analysis out for the two cerebellar hemispheres and the midline using the ROI intensity and the intensity of the activated voxels, in separate analyses. The results obtained were the same for both of these signals, as follows. At time lags $\tau = 0$ or $\tau = 2$, no significant effects were found. However, at $\tau = 1$, statistically significant effects of hand position and velocity (but not of acceleration) were found for all 3 cerebellar ROIs. These results reinforce the relations to speed documented above and also add the position as another significant variable. (Because the shapes drawn are closed, the average X–Y position over the 45-s copying period did not really vary among shapes and thus the effect of position could not be tested in the analysis that was based on data from the whole 45 s.)

Factor analysis

We carried out the factor analysis on the ipsilateral cerebellum because this area showed the strongest effect. The data analyzed consisted of a 20 (rows = subjects) × 9 (columns = shapes) matrix containing the difference in the BOLD signal between copying and visual presentation periods; these data were adjusted for the effect of peak segment speed. Two matrices were analyzed, one containing average ROI data and the other containing the average intensity of the activated voxels. Analysis of the ROI matrix yielded just one factor and thus the analysis was terminated at that stage. However, the analysis of the activated voxel matrix yielded 3 factors (out of 9 possible), which accounted for 100% of the variance in the data, with eigenvalues of 6.4, 1.6, and 0.95, respectively. These results show that there was a grouping of the activation corresponding to the different shapes into 3 groups, whereas the fact that 100% of the variance was accounted for by 3 factors indicates that there was a substantial dimension reduction effected by the factor analysis.

The next step was to identify the group membership of the different shapes. For this purpose we used the direct oblimin factor rotation. The results are shown in Table 6. Factor 1 constituted mostly rounder shapes (hexagon, circle, square, pentagon), which loaded positively and maximally on this factor. In addition, the diamond and equilateral triangle had a partial positive loading on factor 1 (their maxima were on factor 3), whereas there were no negative loadings. Factor 2 constituted one, very elongated, upward pointing shape (isosceles triangle) with maximal positive loading and the vertical lemniscate with smaller partial loading. Interestingly, these 2 downward pointing shapes (vertical trapezoid and diamond) had negative loadings on this factor. Finally, factor 3 constituted upward pointing but less-elongated shapes (vertical lemniscate, equilateral triangle, vertical trapezoid, diamond) with maximal positive loadings and the upward pointing pentagon with a partial positive loading, whereas the more rounded hexagon loaded negatively on this factor. The multiple and signed (positive or negative) loadings of some shapes above is reflected in the nonzero correlation among the 3 factors, and especially in the positive correlation between factors 1 and 3 and the negative correlation between factors 2 and 3 (Table 7). The signed shape membership in the 3 factors is illustrated in Fig. 10. The pattern of loadings derived suggests the following tentative interpretation of the 3 factors. Factor 1 seems to reflect "roundness," factor 2 "upward pointing," and factor 3 "pointing (up or down) and elongation." These results link cerebellar activation to more global, spatial aspects of copying, reminiscent of Bernstein's topological classes (Bernstein 1935).

TABLE 6. *Group membership for the three factors extracted*

Shape	Factor 1	Factor 2	Factor 3
Equilateral triangle	0.202		0.864
Isosceles triangle		1.007	
Square	0.883		
Diamond	0.444	−0.300	0.590
Vertical trapezoid		−0.401	0.757
Pentagon	0.826		0.260
Hexagon	1.096		−0.220
Circle	0.898		
Vertical lemniscate		0.216	1.066

Values indicate factor loadings >0.2.

TABLE 7. *Factor correlations for rotated factors*

	Factor 1	Factor 2	Factor 3
Factor 1	1.000		
Factor 2	−0.048	1.000	
Factor 3	0.537	−0.201	1.000

DISCUSSION

Methodological considerations

In this study we sought to determine the effects that looking at shapes and copying them (without visual feedback) had on the functional activation of the cerebellum, and to describe the relations, if any, between this activation and stimulus- or movement-related parameters. Most of the statistical tests per-

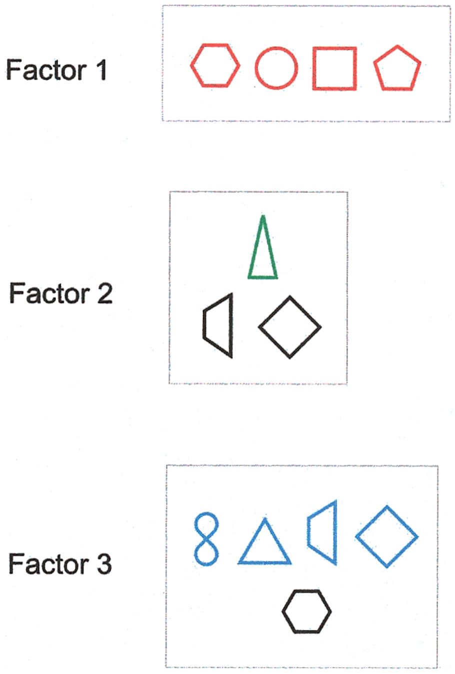

FIG. 10. Color-coded factor membership. Black indicates negative loadings.

formed were based on planned comparisons dictated by the experimental design and, because the design included a number of factors and several quantitative measures of activation, several results were obtained. Finally, it should be noted that all parametric statistical analyses were performed on log-transformed data. The need for this transformation is discussed elsewhere (Lewis et al. 2002).

Behavioral considerations

Shapes were copied continuously and without visual feedback. Overall, the copies produced resembled the templates presented. In general, motor trajectories were segmented, as expected based on previous studies (e.g., Abend et al. 1982; Lee et al. 1997; Novak et al. 2002). Therefore a large part of our analyses was based on the movement segment as the unit of analysis. Of the various movement parameters computed, 3 were least correlated and thus were used as independent variables in regression analyses: length, direction in space (from which the intersegment angular change was computed), and peak speed. Because all shapes were drawn continuously for 45 s, many segments were contained within this period. Therefore average (for the 45-s period) values of these measures were calculated and used for these analyses. Interestingly, the average peak segment speed did not vary significantly among shapes, in contrast to variations in segment length and direction. Finally, it should be noted that, in addition to the spatial trajectories, several motor aspects of the drawings differed appreciably among shapes. This is of particular interest given that the factor shape did not have a significant effect on cerebellar activation.

Cerebellar activation

EFFECT OF VISUAL STIMULATION. In the ROI analysis, no significant activation was found during visual presentation, compared with the rest period. However, activated voxels were found, mainly in the ipsi- and contralateral cerebellum (Table 3), and their average intensity as well as their extent of activation were comparable to, although smaller than, that observed during motor execution. This result is in accord with the finding of cerebellar activation during imagined tennis movements (Decety et al. 1990) and of bilateral cerebellar activation following a cue in a sequential finger-movement task (Cui et al. 2000). This "visual" activation may actually reflect a covert rehearsal of the upcoming copying. This idea is supported by 2 other findings. First, the Talairach coordinate distributions—or, equivalently, the distributions with respect to cerebellar lobules—were very similar for the visually and motorically activated voxels (Fig. 9) and second, the activation during visual presentation was significantly and positively correlated with the speed of the upcoming movement. Of course, other factors, including anticipation of the sensory consequences of the upcoming movement (Miall 1998), could also be involved. In fact, the visual presentation period in the present study can be regarded as an instructed delay period preceding motor execution. In neurophysiological experiments, changes in cell activity during such a delay period have been observed in the cerebellum and in several other motor structures, including the primary motor, premotor, and supplementary motor areas (reviewed in Georgopoulos 1991). In addition, motor set–related activity has been described in the deep cerebellar nuclei (Strick 1983; Thach 1978). A detailed analysis of the patterns of changes in cell activity in an instructed delay period in the motor cortex (Georgopoulos et al. 1989) identified cells that changed activity during both the delay and the movement periods, and others that changed activity only during the movement period. The present results are very similar: certain voxels became activated during both the visual presentation (i.e., instructed delay) period *and* during movement, whereas other voxels apparently were activated, to various degrees, during motor execution.

EFFECT OF MOVEMENT SPEED. Compared with looking at shapes, there was a strong effect of copying them. The effect was present in all 3 ROIs and in all 3 measures of activation. However, the activation was strongest in the ipsilateral cerebellum and half as strong in the contralateral and midline cerebellum. Movement speed had a major impact on the activation observed. Specifically, of all three motor parameters tested (average segment length, change in direction, and peak speed), only the average peak speed had a significant effect. The speed effect was strongest in the ipsilateral cerebellum, and less strong in the contralateral and midline cerebellum. The strong relation between ipsilateral cerebellar activation and movement speed is in accord with known cerebellar connectivity and physiology. The ipsilateral cerebellum is reciprocally connected to the contralateral motor cortex and thus constitutes the main part expected to have a strong relation to motor function. The relations of the ipsilateral cerebellar hemisphere to movement have also been well documented (Brooks and Thach 1981). In addition, a relation of simple spike activity in the ipsilateral cerebellum to movement speed has been well documented in single-cell recording studies in behaving monkeys (Coltz et al. 1999; Johnson and Ebner 2000; Mano and Yamamoto 1980) and in human PET studies (Turner et al. 1998). It is not clear whether this apparent relation to speed reflects a relation to the movement parameter itself, to the strength of muscular activity that underlies the variation in speed, to the sensory inflow to the cerebellum from the moving limb, or to an anticipation of the sensory consequences of the movement (Miall 1998). It is possible that all of these factors are involved. In addition, peak speed is closely related to acceleration. In our sample, the correlation coefficient between the average peak speed and the average acceleration (per 45-s period) was 0.94. (The ultimate selection of the peak speed over acceleration in our analyses was based on its better relation to cerebellar activation in the stepwise multiple regression model used.) Therefore these parameters cannot really be dissociated. A safe interpretation of these findings is that the ipsilateral cerebellum is concerned with dynamic aspects of motor control.

Similarly to the ipsilateral cerebellum, we found significant relations to speed in the contralateral and the midline cerebellum (in the ROI analyses). To our knowledge, there have been no reports of relations of the contralateral cerebellum to motor function in single-cell recordings because such studies have been carried out exclusively on the ipsilateral cerebellum, based on the anatomical connectivity mentioned above. However, activation of the ipsilateral motor cortex has been demonstrated in human fMRI studies (Kim et al. 1993a,b). Considering the connections between the ipsilateral motor cortex and the contralateral cerebellum, as well as the observed activation of the contralateral cerebellum during movement (Cui et al. 2000; Ellermann et al. 1994), our present findings are readily interpretable. Interestingly, the strength of the relation to peak movement speed, as judged by the magnitude of the slope in the regression model, was twice as high in the ipsi- than in the contralateral cerebellum. This provides additional validation to the overall scheme of cerebellar involvement in motor control. Miall et al. (2000, 2001) also measured cerebellar activation during visual and motor tasks but with an emphasis on the effects of coordinated movement between the eyes and hand. Their tasks used both an eye-tracking and hand-tracking paradigm that differ significantly from our study principally in the presence of visual feedback and an investigator-controlled unpredictable path. Therefore comparisons are difficult.

Drawing a figure was also performed in a study by van Mier et al. (1998). Subjects traced mazes, both novel and practiced, as well as a square. The task differed significantly from our study in that the figures were traced using a pen guided by a cutout template. The pen was positioned by the investigator and the movement direction told to the subject. As the subject performed the experiment with eyes closed, no visual feedback was given and no visual template was available during performance. However, there was significant sensory feedback from the figure guide. Finally, the speed of drawing was given to the subject along with instructions on direction changes and touching the sides of the figure. Given this and the difference in techniques, comparisons to our study are difficult, although the greatest similarities occur in the tasks involving the square and the learned maze. Activation, during performance by the right hand, was reported in the ipsilateral anterior cerebellum, ipsilateral dentate, ipsilateral posterior cerebellum, contralateral posterior lateral cerebellum, and contralateral lateral cerebellum. The authors concluded that the first 3 areas relate to a "capacity" effect with the level of activation corresponding to the subject performing at or near capacity. The activation in the contralateral lateral cerebellum was reported to be practice-related. None of the activation in the cerebellar areas was reported to be velocity-related, although in a direct comparison between slow and fast square tracing, cerebellar activation increased during fast tracing in the first 3 areas described above. However, because increases were found for other comparisons, it was concluded that the increase was related to the capacity effect. Overall, the areas involved were similar to those reported in this study, with strong ipsilateral activation across much of the cerebellar hemisphere, but also evidence of contralateral activation. However, a significant difference lies in the lack of reported midline activation in the study by van Mier et al. (1998) and in the absence of a relationship between velocity and activation in the cerebellum. This might be explained by the differences in task and spatial overlap in activation, within the limits of the technique, between velocity and task effects.

TIME COURSE ANALYSIS. This analysis yielded 4 major results. First, significant relations were found only when the movement parameters were regressed against BOLD activation 3 s later. This is in accord with known delays in hemodynamic function (Kwong et al. 1992) and provides a validation to this kind of analysis. Second, significant relations were found in all 3 cerebellar ROIs, which is consistent with the other findings of our study. Third, significant relations were found for velocity as well as for position but not for acceleration. The significant relation to velocity extended the main finding of this study to a finer temporal domain. The relation to position is in accord with findings in the monkey (van Kan et al. 1993) in which significant relations were described between position of the arm and steady-state activity in the mossy fibers. Finally, the lack of significant relations to acceleration is somewhat puzzling, given the known role of cerebellum in force production (Brooks and Thach 1981). In fact, a possible confounding factor with respect to the speed effect is the strength of muscle activation, which covaries with speed. For example, it has been shown that neural activity in the magnocellular part of the red nucleus that is apparently correlated with the speed of the movement is also highly correlated with muscle activation (Miller and Houk 1995). Similarly, clear relations between Purkinje cell activity and muscle activity has been reported (Miller et al. 2002). These considerations are in accord with the long-standing association of cerebellar function to the strength of muscle contraction, dating back to Luciani ("sthenic neuromuscular effect," see Luciani 1915, p. 471; Luciani also discussed previous ideas on the role of the cerebellum in muscle activation). Now, if this were the case, one would have expected to find a significant relation between cerebellar activation and acceleration, which was not found. Instead, significant relations to velocity and position was observed. In fact, these relations resemble those found in the motor cortex in neurophysiological experiments (Ashe and Georgopoulos 1994), an area with which cerebellum is interconnected; that is, strong relations to velocity and position but not acceleration (Ashe and Georgopoulos 1994).

Localization of motor copying effects

The presence of a significant relation to peak segment speed was used as an indicator to determine the potentially differential localization of motor relations in the cerebellum during copying. In addition, the magnitude of the slope in *Eq. 4* (or, equivalently, of the exponent in *Eq. 5*) was taken as an indicator of the strength of the relation. The localization data were evaluated from 2 perspectives stemming from the known anatomical organization of the cerebellum (Voogd and Glickstein 1998), that is, the anteroposterior organization in lobules and the mediolateral organization in zones. The former is mostly based on anatomical features, whereas the latter reflects the organization of the cerebellar cortical output onto the deep cerebellar nuclei. With respect to the anteroposterior hemispheric localization, statistically significant relations were observed only in the ipsilateral hemisphere in which there was a clear gradient of increasingly stronger relations from anterior (absent in lobules I–VI) to posterior (strongest in lobules VIIB–X). Even in the contralateral (left) hemisphere, there was a similar gradient of the P values of the speed effect from anterior to posterior, although these values did not reach statistical significance.

The distribution of the speed effect in mediolateral zones was very interesting. First, there was a highly significant and strong relation in the vermis (midline) where the slope was close in magnitude to that observed in the posterior ipsilateral lobules. This indicates a clear involvement of the vermis in dynamics of arm movements and could reflect peripheral proprioceptive inputs (Bloedel and Courville 1981). Second, there was a significant but relatively weak (in terms of the magnitude of the slope) relation in the paramedian zones of both hemispheres. Third, a very strong relation was observed in the ipsilateral lateral zone where the slope actually reached the highest value in this analysis (Table 5); in contrast, no significant relation was found in the lateral zone of the contralateral hemisphere. These findings are in accordance with the original observations by Holmes (see Phillips 1979) on patients with gunshot wounds in the lateral aspects of the hemisphere, which documented clear motor deficits. On the whole, then, our results documented a specific, highly significant, and well-localized involvement of the cerebellar cortex to peak movement speed. They also documented the importance of the mediolateral zones in this function, given that this organization revealed the strongest relation (in the ipsilateral hemisphere) and also the presence of the relation in the contralateral hemisphere.

The nature of this relation to peak speed must be interpreted in multiple contexts, including afferent input, motor output, and their complex interactions. It is well known that the cerebellum receives massive afferent input from the somatic periphery (Bloedel and Courville 1981), is intimately involved in movement initiation and control (Brooks and Thach 1981), and is hypothesized to be involved in processing anticipated sensory consequences of motor actions (Blakemore et al. 2001; Miall 1998). The speed of movement is an essential motor parameter and is likely to be prominent in all of these aspects of motor control and, because the fMRI integration time is in the order of seconds, it is reasonable to suppose that the observed relations reflect all of these factors. Finally, a surprising aspect of the present findings was the lack of significant relations to a host of other motor parameters that varied substantially among the motor shape trajectories drawn. This underscores the specificity of cerebellar involvement in motor control amid a wide variety of inputs, outputs, and connections with other brain regions.

Spatial aspects of copying

Although the average activation did not differ significantly among shapes, it was nevertheless correlated between shapes to varying degrees, especially with respect to the intensity of the activated voxels. This suggested that the 9 shapes could be reduced to a smaller number of aggregate shapes. For that purpose, we used factor analysis. This is an exploratory data analysis technique that aims to identify latent factors underlying the correlations among variables. In the present application, a factor analysis of principal components yielded a reduction of the 9 shapes into 3 groups. The general characteristics of the shapes making up these groups (red, green, and blue shapes in Fig. 10) suggest 3 basic principles of grouping: roundness, elongation, and pointing. The group membership derived indicates that factor 1 reflects roundness, whereas factors 2 and 3 are composites with respect to elongation and pointing. Specifically, factor 2 is dominated by upward pointing, as evidenced not only by the positive loading of the isosceles triangle but also by the negative loading of the only 2 shapes that point downward (diamond and vertical trapezoid). Factor 3 seems to reflect mostly elongation and/or pointing in either the up or down direction. These results link cerebellar activation to more global, spatial aspects of copying, reminiscent of Bernstein's topological classes (Bernstein 1935). This association of cerebellar activation with higher-order spatial aspects of copying is consistent with the findings of Shimansky et al. (1997), which demonstrated that patients with cerebellar lesions are deficient in drawing an accurate representation of the template even under full vision, although these patients were more impaired when drawing a shape with which they were acquainted through kinesthetic cues.

DISCLOSURES

This work was supported by National Institutes of Health Grants NS-32919 and RR-088079, the University of Minnesota Graduate School (T. A. Jerde), the United States Department of Veterans Affairs, and the American Legion Chair in Brain Sciences.

REFERENCES

Abend W, Bizzi E, and Morasso P. Human arm trajectory formation. *Brain* 105: 331–348, 1982.

Asanuma C, Thach WT, and Jones EG. Distribution of cerebellar terminations and their relation to other afferent terminations in the ventral lateral thalamic region of the monkey. *Brain Res Rev* 5: 237–265, 1983a.

Asanuma C, Thach WT, and Jones EG. Anatomical evidence for segregated focal groupings of efferent cells and their terminal ramifications in the cerebellothalamic pathway of the monkey. *Brain Res Rev* 5: 267–297, 1983b.

Ashe J and Georgopoulos AP. Movement parameters and neuronal activity in motor cortex and area 5. *Cereb Cortex* 6: 590–600, 1994.

Bernstein N. The problem of interrelation of co-ordination and localization. *Arch Biol Sci* 38: 1935. (Reproduced in: *Human Motor Actions*, edited by Whiting HTA. Amsterdam: North-Holland, 1984, p. 77–119.)

Blakemore SJ, Frith CD, and Wolpert DM. The cerebellum is involved in predicting the sensory consequences of action. *Neuroreport* 12: 1879–1884, 2001.

Bloedel JR, Bracha V, Milak M, and Shimansky Y. Cerebellar contributions to the acquisition and execution of learned reflex and volitional movements. *Prog Brain Res* 114: 499–509, 1997.

Bloedel JR and Courville J. Cerebellar afferent systems. In: *Handbook of Physiology. The Nervous System. Motor Control.* Bethesda, MD: Am. Physiol. Soc., 1981, sect. 1, vol. II, pt. 2, chapt. 16, p. 735–831.

Brooks VB and Thach WT. Cerebellar control of posture and movement. In: *Handbook of Physiology. The Nervous System. Motor Control.* Bethesda, MD: Am. Physiol. Soc., 1981, sect. 1, vol. II, pt. 2, chapt. 18, p. 877–947.

Coltz JD, Johnson MT, and Ebner TJ. Cerebellar Purkinje cell simple spike discharge encodes movement velocity in primates during visuomotor arm tracking. *J Neurosci* 19: 1782–1803, 1999.

Cox RW and Jesmanowicz A. Real-time 3D image registration for functional MRI. *Magn Reson Med* 42: 1014–1018, 1999.

Cui SZ, Li EZ, Zang YF, Weng XC, Ivry R, and Wang JJ. Both sides of human cerebellum involved in preparation and execution of sequential movements. *Neuroreport* 11: 3849–3853, 2000.

Decety J, Sjoholm H, Ryding E, Stenberg G, and Ingvar DH. The cerebellum participates in mental activity: tomographic measurements of regional cerebral blood flow. *Brain Res* 535: 313–317, 1990.

Draper NR and Smith N. *Applied Regression Analysis.* New York: Wiley, 1981.

Dum RP and Strick PL. An unfolded map of the cerebellar dentate nucleus and its projections to the cerebral cortex. *J Neurophysiol* 89: 634–639, 2003.

Ebner TJ. A role of the cerebellum in the control of limb movement velocity. *Curr Opin Neurobiol* 8: 762–769, 1998.

Efron B and Tibshirani RJ. *An Introduction to the Bootstrap.* New York: Chapman & Hall, 1993.

Ellermann JM, Flament D, Kim S-G, Fu Q-G, Merkle H, and Ebner TJ. Spatial patterns of functional activation of the cerebellum investigated using high field (4T) MRI. *NMR Biomed* 7: 63–68, 1994.

Gao JH, Parsons LM, Bower JM, Xiong J, Li J, and Fox PT. Cerebellum implicated in sensory acquisition and discrimination rather than motor control. *Science* 272: 545–547, 1996.

Georgopoulos AP. Higher order motor control. *Annu Rev Neurosci* 14: 361–377, 1991.

Georgopoulos AP, Crutcher MD, and Schwartz AB. Cognitive spatial motor processes. 3. Motor cortical prediction of movement direction during an instructed delay period. *Exp Brain Res* 75: 183–194, 1989.

Gilman S, Bloedel J, and Lechtenberg R. *Disorders of the Cerebellum.* Philadelphia, PA: FA Davis, 1981.

Green P. *Analyzing Multivariate Data.* Hinsdale, IL: Dryden Press, 1978.

Imamizu H, Miyauchi S, Tamada T, Sasaki Y, Takino R, Putz B, Yoshioka T, and Kawato M. Human cerebellar activity reflecting an acquired internal model of a new tool. *Nature* 403: 192–195, 2000.

Ivry RB, Keele SW, and Diener HC. Dissociation of the lateral and medial cerebellum in movement timing and movement execution. *Exp Brain Res* 73: 167–180, 1988.

Johnson MT and Ebner TJ. Processing of multiple kinematic signals in the cerebellum and motor cortices. *Brain Res Rev* 33: 155–168, 2000.

Kahlon M and Lisberger SG. Changes in the responses of Purkinje cells in the floccular complex of monkeys after motor learning in smooth pursuit eye movements. *J Neurophysiol* 84: 2945–2960, 2000.

Kim JJ and Thompson RF. Cerebellar circuits and synaptic mechanisms involved in classical eyeblink conditioning. *Trends Neurosci* 20: 177–181, 1997.

Kim J-O and Mueller CW. *Factor Analysis. Statistical Methods and Practical Issues.* Newbury Park, CA: Sage, 1978.

Kim S-G, Ashe J, Georgopoulos AP, Merkle H, Ellermann JM, Menon RS, Ogawa S, and Uğurbil K. Functional imaging of human motor cortex at high magnetic field. *J Neurophysiol* 69: 297–302, 1993a.

Kim S-G, Ashe J, Hendrich K, Ellermann JM, Merkle H, Uğurbil K, and Georgopoulos AP. Functional magnetic resonance imaging of motor cortex: hemispheric asymmetry and handedness. *Science* 261: 615–617, 1993b.

Kim S-G, Hendrich K, Hu X, Merkle H, and Uğurbil K. Potential pitfalls of functional MRI using conventional gradient-recalled echo techniques. *NMR Biomed* 7: 69–74, 1994a.

Kim S-G, Uğurbil K, and Strick PL. Activation of a cerebellar output nucleus during cognitive processing. *Science* 265: 949–951, 1994b.

Kwong KK, Belliveau JW, Chesler DA, Goldberg IE, Weisskopff RM, Poncelet BP, Kennedy DN, Hoppel BE, Cohen MS, Turner R, Cheng H-M, Brady TJ, and Rosen BR. Dynamic magnetic resonance imaging of human brain activity during primary sensory stimulation. *Proc Natl Acad Sci USA* 89: 5675–5679, 1992.

Lee D, Port NL, and Georgopoulos AP. Manual interception of moving targets. II. On-line control of overlapping submovements. *Exp Brain Res* 116: 421–433, 1997.

Lewis SM, Jerde TA, Tzagarakis C, Tsekos N, Amirikian B, Georgopoulos MA, Kim S-G, Uğurbil K, and Georgopoulos AP. Logarithmic transformation for BOLD fMRI data. *Soc Neurosci Abstr* 506.7, 2002.

Luciani L. *Human Physiology*, edited by Holmes GM. London: Macmillan, 1915, p. 419–485.

Mano N and Yamamoto K. Simple-spike activity of cerebellar Purkinje cells related to visually guided wrist tracking movement in the monkey. *J Neurophysiol* 43: 713–728, 1980.

Miall CR. The cerebellum, predictive control and motor coordination. In: *Sensory Guidance of Movement*, edited by Bock GR and Goode JA. New York: Wiley, 1998.

Miall RC, Imamizu H, and Miyauchi S. Activation of the cerebellum in co-ordinated eye and hand tracking movements: an fMRI study. *Exp Brain Res* 135: 22–33, 2000.

Miall RC, Reckess GZ, and Imamizu H. The cerebellum coordinates eye and hand tracking movements. *Nat Neurosci* 4: 638–644, 2001.

Miller LE, Holdefer RN, and Houk JC. The role of the cerebellum in modulating voluntary limb movement commands. *Arch Ital Biol* 140: 175–183, 2002.

Miller LE and Houk JC. Motor co-ordinates in primate red nucleus: preferential relation to muscle activation *versus* kinematic variables. *J Physiol* 488: 533–548, 1995.

Novak KE, Miller LE, and Houk JC. The use of overlapping submovements in the control of rapid hand movements. *Exp Brain Res* 144: 351–364, 2002.

Oldfield RC. The assessment and analysis of handedness: the Edinburgh inventory. *Neuropsychologia* 9: 97–113, 1971.

Phillips CG. *Selected Papers of Gordon Holmes.* New York: Oxford Univ. Press, 1979.

Schmahmann JD, Doyon J, Toga AW, Petrides M, and Evans AC. *MRI Atlas of the Human Cerebellum.* San Diego, CA: Academic Press, 2000.

Shimansky Y, Saling M, Wunderlich DA, Bracha V, Stelmach GE, and Bloedel JR. Impaired capacity of cerebellar patients to perceive and learn two-dimensional shapes based on kinesthetic cues. *Learn Mem* 4: 36–48, 1997.

Snedecor GW and Cochran WG. *Statistical Methods.* Ames, IA: Iowa State Univ. Press, 1989.

Strick PL. The influence of motor preparation on the response of cerebellar neurons to limb displacements. *J Neurosci* 3: 2007–2020, 1983.

Talairach J and Tournoux P. *Co-planar Stereotaxic Atlas of the Human Brain.* New York: Thieme, 1988.

Thach WT. Correlation of neural discharge with pattern and force of muscular activity, joint position, and direction of intended next movement in motor cortex and cerebellum. *J Neurophysiol* 41: 654–676, 1978.

Thach WT. A role for the cerebellum in learning movement coordination. *Neurobiol Learn Mem* 70: 177–188, 1998.

Thach WT, Goodkin HP, and Keating JG. The cerebellum and the adaptive coordination of movement. *Annu Rev Neurosci* 15: 403–442, 1992.

Turner RS, Grafton ST, Votaw JR, Delong MR, and Hoffman JM. Motor subcircuits mediating the control of movement velocity: a PET study. *J Neurophysiol* 80: 2162–2176, 1998.

van Kan PL, Gibson AR, and Houk JC. Movement-related inputs to intermediate cerebellum of the monkey. *J Neurophysiol* 69: 74–94, 1993.

van Mier H, Tempel LW, Perlmutter JS, Raichle ME, and Petersen SE. Changes in brain activity during motor learning measured with PET: effects of hand of performance and practice. *J Neurophysiol* 80: 2177–2199, 1998.

Voogd J and Glickstein M. The anatomy of the cerebellum. *Trends Neurosci* 21: 370–375, 1998.

Winstein CJ, Grafton ST, and Pohl PS. Motor task difficulty and brain activity: investigation of goal-directed reciprocal aiming using positron emission tomography. *J Neurophysiol* 77: 1581–1594, 1997.